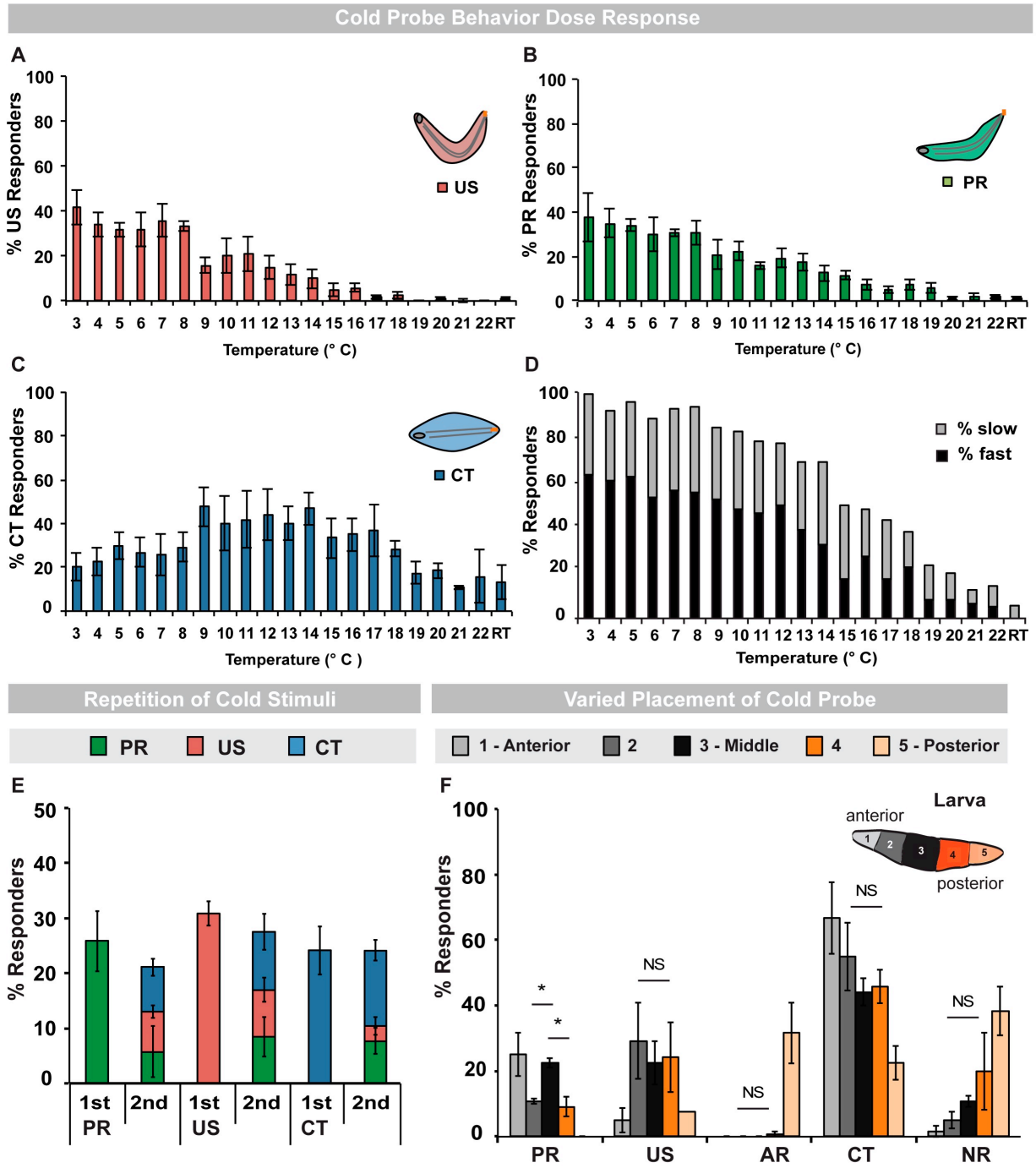

Figure S1. Characteristics of cold probe assay response, related to Figure 1. (A) Percentage of US, (B) PR and (C) CT in response to cold probe at various temperatures averaged ± s.e.m.. (D) Latency of all responses to cold probe with respect to temperature. Fast = response within 3 s of onset of cold stimulus; slow = response 4-10 s after onset of cold stimulus. (E) Behavioral responders to cold probe (6 °C) during initial stimulus (1st) were separated based on response and tested with a second 'follow up' stimulus (2nd). (F) Larval behavioral responses where the cold probe (6 °C) was applied to multiple mid regions of larvae (1-5). Colors indicate placement of the probe from anterior to posterior: 1 = on the most anterior segments; 2 = inbetween the most anterior and middle of larva, 3 = in the middle-most segment; 4 = inbetween the middle and posterior end; and 5 = on the posterior end. PR = posterior raise; US = U-shape; AR = anterior raise; CT = contraction; and NR = non-responder. (A-F) n = 3 sets of 40 larvae averaged ± s.e.m..

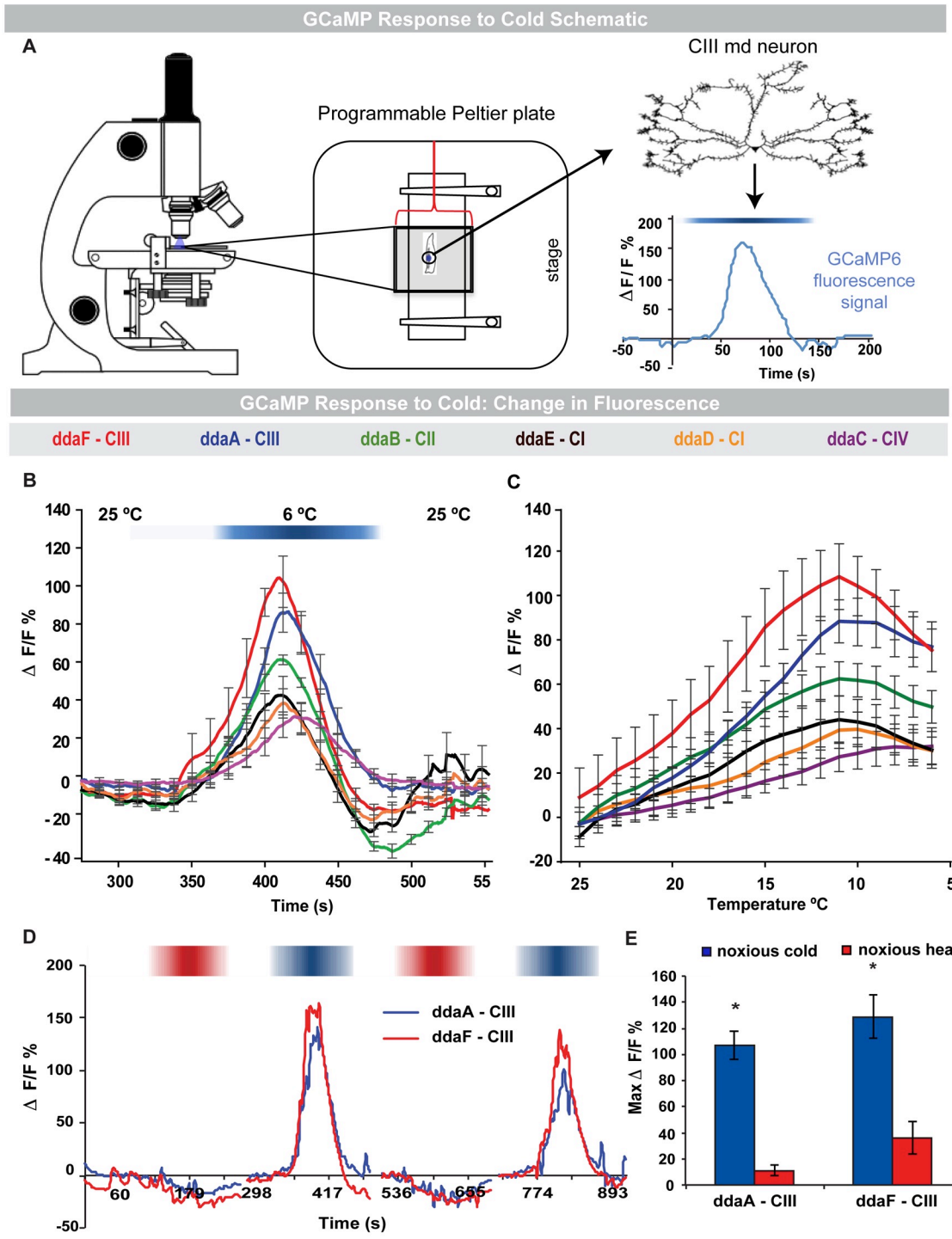

Figure S2. Class III neurons are most specifically activated by cold via GCaMP signaling assay, related to Figure 2. (A) Diagram of time-lapse live imaging of GCaMP6 activation in response to cold stimulation. Intact third instar larvae are immobilized and placed on a programmable Peltier cold plate (boxed region in middle inset) under a confocal microscope. Shown here is a class III neuron identified under the microscope via expression of fluorescent transgenes, cell body shape and specific location in the larval segment. The Peltier plate is then cooled (6 °C) from a baseline control temperature (25 °C) while the change in GCaMP6 fluorescence signal in specific sensory neurons is recorded as a change in fluorescence over baseline over time. Blue bar indicates cooling of the plate over time, with coldest temperature shown in darkest blue. (B) Averaged GCaMP responses in md neurons with application of cold stimulus over time. White-blue spectrum bar signifies temperature range (25-6 ˚C, coldest

temperature tested being the dark blue region), n = 20 per neuron type. (C) Averaged max change in fluorescence at a range of ambient to cold temperatures (25-6 ºC) in different classes of sensory neurons, n = 20 per neuron type. (D) Representative tracing of GCaMP6 responses in class III neurons subjected to alternating noxious heat (44 ˚C) and noxious cold (6 ˚C) temperature cycles, n = 10. (E) Quantification of GCaMP activation in dorsal class III neuron subtypes (ddaA, ddaF) in response to cold (6 ˚C) vs hot (44 ˚C) stimuli. A two-tailed Welch's t-test was used to assess differences in average peak $\Delta F/F$ % ± s.e.m under noxious cold and heat exposure, * = $p < 0.001$, n = 10 per neuron subtype and condition. (B, C, E) Error bars represent ± s.e.m..

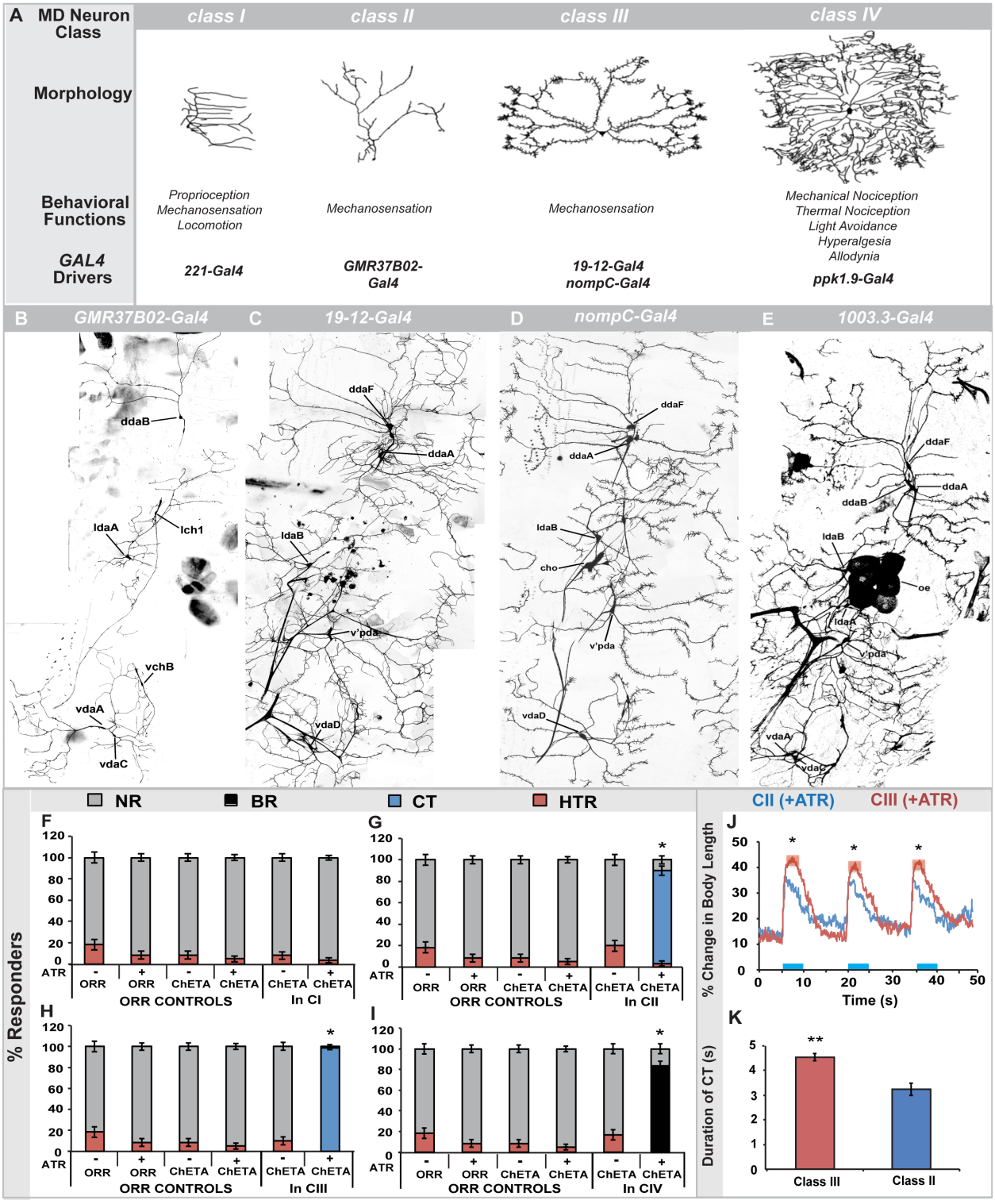

Figure S3. md sensory neuron classes: morphology, functions and drivers and optogenetic activation of CT response is specific to class II and III neurons, related to Figure 3. (A) Representative images of md neuron dendritic morphology shown with known behavioral functions for each class and *Gal4* drivers that mediate class-specific expression. (B-E) Larval hemisegment expression of *UAS-mCD8::GFP* with (B) class II (*GMR37B02-Gal4*); (C) class III (*19-12-Gal4*) (D); class III (*nompC-Gal4*) and (E) class II and III (*1003.3-Gal4*) drivers in live epidermal whole mounts. (B-E) CII neurons: ddaB, ldaA, vdaA, vdaC; CIII neurons: ddaF, ddaA, ldaB, v'pda,

vdaD; chordotonal neurons: lch1, vchB, cho; oenocytes: oe. (F) Behavioral responses observed upon optogenetic activation of class I (CI x ChETA), (G) class II (CII x ChETA), (H) class III (CIII x ChETA) and (I) class IV (CIV x ChETA) neurons. (F-I) The control strain (ORR), channelrhodopsin alone (ORR x CHETA), or larvae lacking the required ATR cofactor (-ATR) served as negative controls. HTR= head and/or tail raise; CT = contraction; BR = body roll; NR = non-responder. n = 15-20 per genotype/condition averaged ± s.e.p.. (J) Change in body length during optogenetic activation of class II or III neurons. Shaded red boxes indicate time period in which larvae exhibit a significantly increased change in body length in class III vs. class II. Light blue boxes indicate duration of 480 nm blue light stimulation. (K) Average duration of optogenetically-induced CT behavior (seconds) in class III vs. class II md neurons ± s.e.m.. Stats: (F-I) A two-tailed Fisher's exact test with Bonferonni correction, * = $p < 0.0001$, (J-K) A two-tailed Welch's t-test, * = $p < 0.05$, ** = $p < 0.001$, n = 20 per genotype. (J-I) error bars represent ± s.e.p..

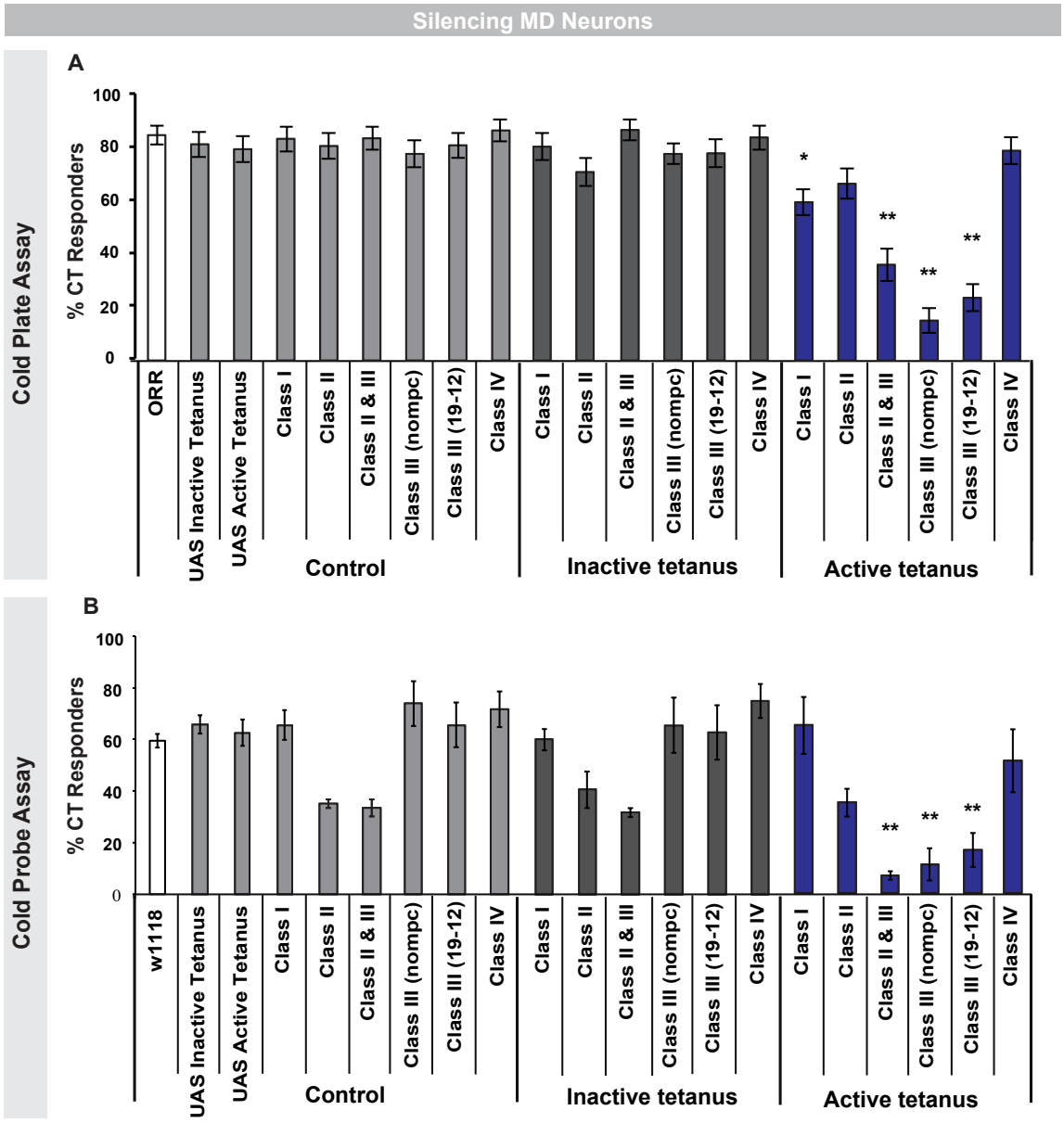

Figure S4. Class III neurons are required for cold-evoked CT behavior, related to Figure 4. (A-B) Percent contraction responders observed upon silencing md neurons in a class-specific manner via an active tetanus toxin transgene in the (A) cold plate (6 ˚C), and (B) cold probe assay (11 °C). For cold plate, n = 60-100 larvae per genotype averaged ± s.e.p.. For cold probe assay, n = 3 sets of 40 larvae were averaged ± s.e.m.. White and grey bars indicate controls, blue bars indicate class-specific silencing with tetanus toxin transgene expression. Stats: two-tailed Fisher's exact test with Bonferroni correction, * = $p < 0.0125$, ** = $p < 0.0001$.

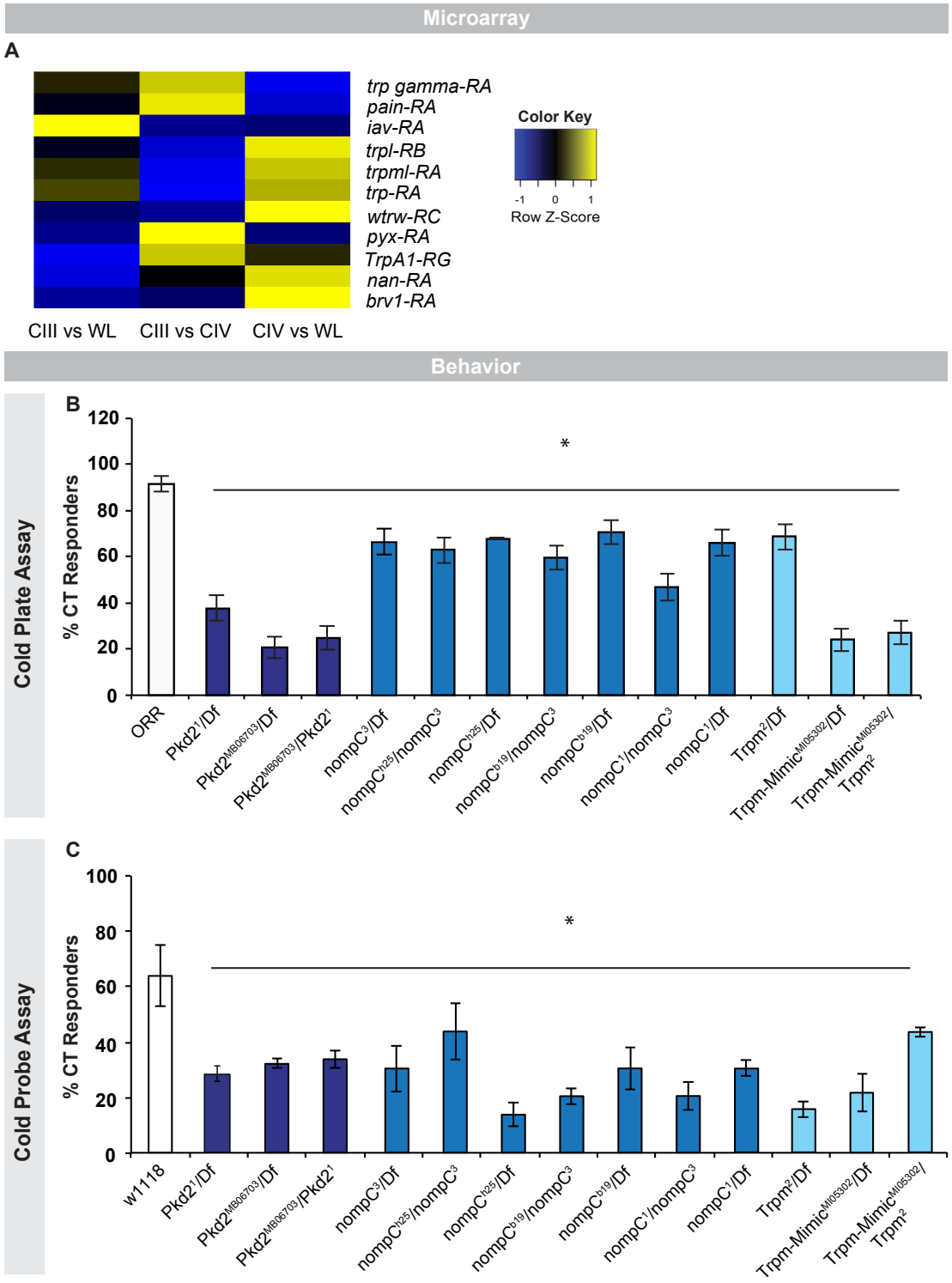

Figure S5. Expression and function of TRP channel genes in cold nociception, related to Figure 5.
(A) Microarray comparing TRP gene isoforms in CIII vs. CIV neurons, CIII vs. whole larva (WL) or CIV vs. WL. Color key: degree of enrichment, yellow being more enriched and blue not enriched by comparison. (B) CT

responses in larvae expressing *Pkd2, Trpm,* or *nompC* mutant alleles in the cold plate (6 ºC, n = 61-72 except *nompC[h25]/Df* where n = 25, larvae, responses averaged ± s.e.p.), and (C) cold probe (10 ºC, n = 60 larvae averaged ± s.e.m.) assay, (B-C) White bar represents control responses; colored bars indicate different targeted genes. * = $p < 0.05$.

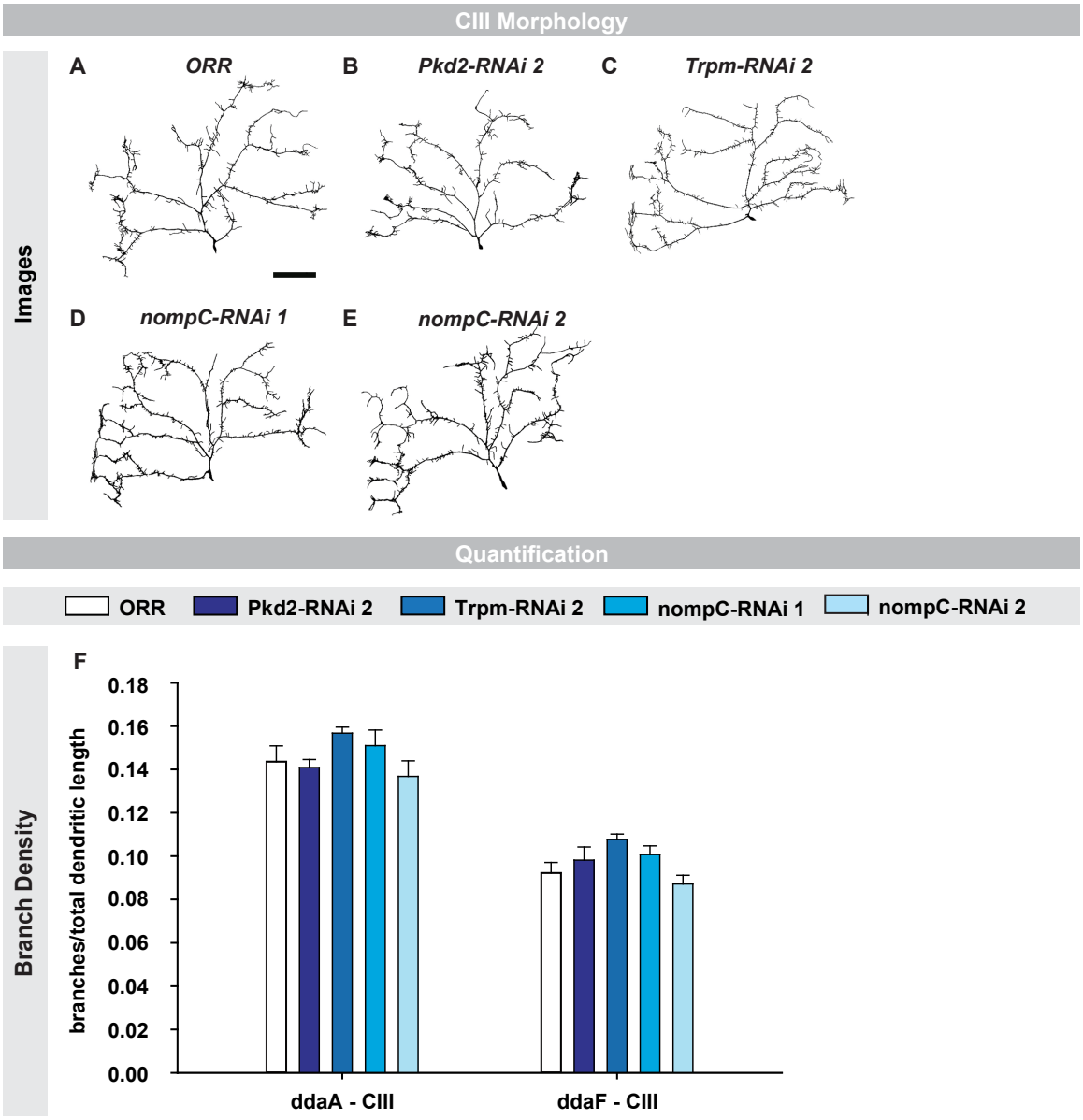

Figure S6. Larvae with class III neurons expressing TRP channel RNAi transgenes have normal dendritic morphology, related to Figure 5. Dendritic morphology of class III sensory neurons (ddaF) expressing RNAi transgenes: (A) control (ORR), (B) Pkd2-RNAi 2, (C) Trpm-RNAi 2, (D) nompC-RNAi 1, or (E) nompC-RNAi 2. Gene-specific RNAi transgenes presented here produced significant defects in CT behavior in the cold plate and/or cold probe assay (See Fig. 5C-5D). (F) Quantification of dendritic morphology of class III neuron types (ddaA and ddaF) via comparison of branch density in RNAi expressing neurons compared to control (ORR). Average branch density measured as total branches/total dendritic length ± s.e.m., scale bar represents 100 μm. Stats: two-tailed Welch's t-test with Bonferroni correction, ($p > 0.05$), n = 6-11.

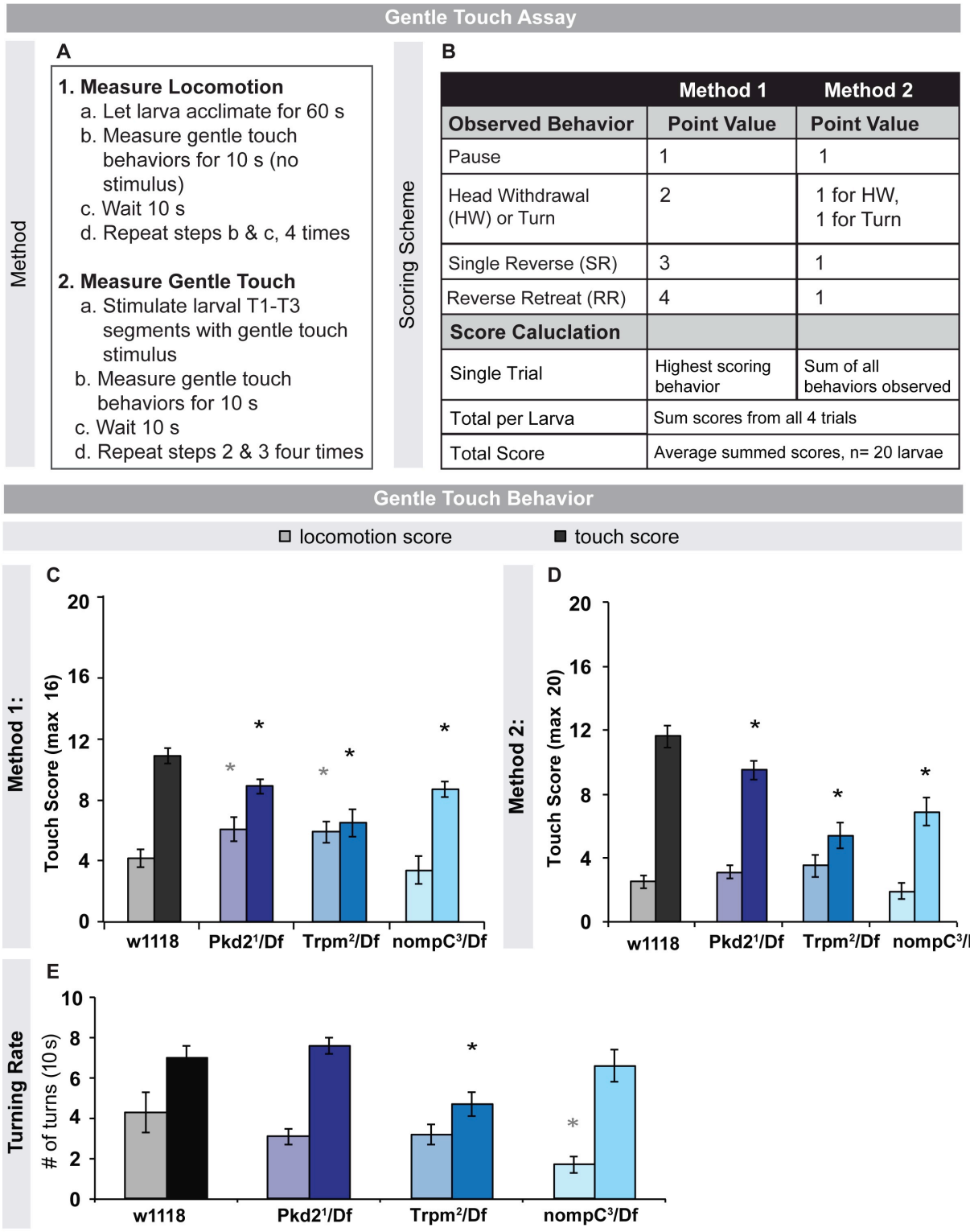

Figure S7. Pkd2, Trpm and NompC mutant larvae exhibit gentle touch defects, related to Figure 7. (A) Diagram of gentle touch assay and (B) scoring schemes used to assess (C, D) locomotion and gentle touch responses in control (grey/black bars) larvae and mutants over relevant deficiencies (colored bars). (E) Comparison of the number of larval turns during normal locomotion or gentle touch trials. (C-E) Bars representing locomotion (light colors) or touch (darker colors) scores were averaged from 10 larvae. Each larvae was tested four times and scores

were summed. Error bars indicate s.e.m.. Stats: two-tailed Welch's t-test * $p > 0.05$ compared to black control bar. * $p > 0.05$ compared to grey control bar.

Supplemental Experimental Procedures

Fly Stocks and Genetics

Drosophila melanogaster larvae were raised on cornmeal food at 25°C. *Oregon R* (*ORR*) and w^{1118} were control strains. Mid-late 3rd instar larvae were used for all behavioral assays, selected based on age and size matching as well as documented developmental markers. Mutants: $Pkd2^{1}$, $Trpm^{2}$ [S1], $nompC^{3}$ [S2] (gift of K. Venkatachalam), $Trpm^{MI05302}$ (gift of H. Bellen), $Pkd2^{MB0670}$, $nompC^{1}$, $nompC^{h25}$, $nompC^{b19}$ were from Bloomington. Deficiencies: *Df(2L)BSC407* (*Pkd2*), *Df(2R)XTE-11* (*Trpm*), and *Df(2L)Exel6012* (*nompC*) were from Bloomington. Gal4 Lines: $Gal4^{2\text{-}21}$ (CI [S3]), *GMR37B02-Gal4* (CII [S4]), *19-12-Gal4* [S5] and *nompC-Gal4* (CIII [S6]), *ppk-Gal4,UAS-mCD8::GFP, ppk-Gal80* (CIII [S7]), $Gal4^{ppk1.9}$ and $Gal4^{477}$;$Gal4^{ppk1.9}$ (CIV [S8, S9]), *1003.3-Gal4* (CII/CIII [S10]) $Gal4^{21\text{-}7}$ (*md-Gal4,* classes I-CIV [S11]). *19-12-Gal4* was used for all behavioral experiments to drive expression in class III except where indicated (Fig. 4, and Fig. S4). UAS transgenes: *UAS-TeTxLC* (active tetanus toxin [S12]), *UAS-IMP TNT VI-A* (inactive tetanus toxin [S12]), *UAS–GCaMP6m* [S13], *UAS-channelrhodopsin-2* (ChETA-YFP [S6]), *UAS-mCD8::*GFP [S14], *UAS-CaMPARI* [S15], *UAS-nompC-GFP* [S16], *UAS-Pkd2* (gift of X. Lu), *UAS-TrpA1* [S17]. *UAS-RNAi* lines from Vienna *Drosophila* RNAi Center [S18]: 6941 ($UAS\text{-}Pkd2^{RNAi1}$); from TRiP collection [S19]: 31296 ($UAS\text{-}Pkd2^{RNAi2}$), 31672 ($UAS\text{-}Trpm^{RNAi1}$), 35581 ($UAS\text{-}Trpm^{RNAi2}$), 31291 ($UAS\text{-}Trpm^{RNAi3}$), 31689 ($UAS\text{-}nompC^{RNAi1}$), 31512 ($UAS\text{-}nompC^{RNAi2}$), 31676 ($UAS\text{-}para^{RNAi\ 1}$), and 33923 ($UAS\text{-}para^{RNAi\ 2}$).

Local cold probe assay

The custom built probe (ProDev Engineering, Figure 1C) consists of a temperature controlled Peltier device which cools the aluminum shaft, a thermistor (TE Technologies, Inc.) embedded inside the rounded conical tip, and a heat sink/fan to maintain the desired temperature (22 - 0 °C). The closed loop thermal management system measures and reports real time tip temperature and maintains the setpoint to within a half a degree. The tip tapers from 1.5 mm to a fine point, capable of contacting a single body segment.

Global cold plate assay

Video recordings (30 fps (frames per second) for all transallelic and rescue experiments and 5 fps all other experiments) of first 5 seconds of stimulation were captured and behaviorally assessed. The Skeletonize and Analyze Particles functions in Image J were used to extract larval body length in pixels. For defining a quantitative threshold of CT, we performed cold plate assays with control third instar larvae, and maximum change in larval body length was calculated. Next, we calculated the average and standard deviation of maximum change in body length for larvae. For CT, a threshold percent change in body length was defined as greater than 37%, which equates to the average under cold exposure (6-10ºC) plus 1.5 standard deviations for a larval population.

Heat Probe Assay

The heat probe assay was conducted as previously described [S20]. Briefly, a metal tipped probe heated to 45 °C via electric thermocouple was applied gently to the mid dorsal surface of the larva and held for up to 20 s. A 360 ° body roll response within 5 s was recorded as a fast responder, 6-20 s, a slow responder, and normal locomotion for the full 20 s was recorded as no response [S20].

Gentle Touch Assay

A single larva were first gently placed on an agarose plate under a bright field microscope and allowed to acclimate for 1 minute. The larva was then observed for four 10-second trials (20 seconds apart) without any stimulation to record normal locomotion behaviors (same as gentle touch behaviors outlined below) and the scores were summed. The larva was then gently stimulated with a light brushstroke of a feather in the thoracic segments (T1-T3) and gentle touch behaviors were recorded for 10 seconds. The same larva was tested for gentle touch responses during four 10-second trials 20 seconds apart and the scores were summed. Gentle touch behaviors scored included the following: pause in locomotion (pause), retraction of the anterior segments (HW- head withdrawal), turn of the anterior segments between 45-180º (turn), single reverse wave of body segments (reverse), and multiple reverses in locomotion (retreat). Since "turning" is a behavior that is copiously observed during normal locomotion as well as after a gentle touch stimulus, gentle touch scores during a non-stimulated trial ("locomotion score") were compared for each genotype. Scoring of these behaviors was carried out in two ways: Method 1: Behaviors were

weighted in ascending order such that pause = 1 point, turn or HW = 2 points, reverse = 3 points, retreat = 4 points. Each trial was given a single score depending on the "highest scoring" behavior observed (max total for each trial = 4, over four trials the summed max total score = 16). Method 2: Each behavior was weighted equally (1 point) and all behaviors for a trial were summed (max total for each trial = 5, summed max total score = 20). See schematic in Figures S7A-S7B for a summary outline of these scoring schemes. The number of turns was also recorded during normal locomotion trial and after gentle touch.

***in vivo* calcium imaging**

GAL4^{217}*, UAS-mCD8::RFP* or *19-12-GAL4,UAS-mCD8::RFP* drove the genetically encoded calcium sensor *UAS-GCaMP6*. Live, third-instar larvae were individually immobilized between a glass slide and a 22 x 50 mm glass coverslip then imaged on a Nikon C1 Plus confocal microscope with a Linkam PE 120 Peltier stage and a 20x oil immersion lens. Larvae were subjected to a programmed temperature regiment via the Linkam T95 controller. The noxious cold regiment for pan *md-GAL4* driven *UAS-GCaMP6* expression was as follows: 1. An initial 350 s of 25 ˚C; 2. A ramp down to 6 ˚C at a rate of 20 ˚C/min, holding for 10 s; 3. A ramp up to 25 ˚C at a rate of 20 ˚C/min holding for 120 s, then steps 2-3 repeated. The noxious cold regiment for class III (*19-12-GAL4*) driven *UAS-GCaMP6* expression was as follows: 1. An initial 120 s of 25 ˚C; 2. A ramp down to 6 ˚C at a rate of 20 ˚C/min, holding for 10 s; 3. A ramp up to 25 ˚C at a rate of 20˚C/min holding for 60 s, then steps 2-3 repeated. The alternating noxious heat and noxious cold regiment for class III (*19-12-GAL4*) driven *UAS-GCaMP6* expression was as follows: 1. An initial 90 s of 25 ˚C; 2. A ramp up to 44 ˚C at a rate of 20 ˚C/min, holding for 10 s; 3. A ramp down to 25 ˚C at a rate of 20 ˚C/min, holding for 60 s; 4. A ramp down to 6 ˚C at a rate of 20 ˚C/min, holding for 10 s; 5. A ramp up to 25 ˚C at a rate of 20 ˚C/min, holding for 60 s, then steps 2-5 repeated.

Dorsal da neuron clusters were recorded (256 x 256 pixel resolution, frame interval 620 ms) and motion corrected using Image J plugin *StackReg*. Videos with excessive larval movement were discarded. Mean fluorescence of the neuronal soma was measured using Image J plot z-profile function. Data was smoothed with a 5 frame moving average in the statistical *R* programming language. Max $\Delta F/F_0$ was calculated using ROIs during each ramp down to 6 ˚C or up to 44 ˚C and averaged for each neuron (See Figure 2). F_0 represents average baseline fluorescence 350 s prior to temperature ramp. Average max $\Delta F/F_0$ was compared using Welch's t-test with Bonferonni correction, except for comparisons involving ddaE, which did not meet the assumption of normality where a Mann-Whitney U test with Bonferonni correction was used instead. For cross-correlation analyses, correlation coefficients (Pearson's correlation) were calculated in Microsoft Excel® to examine the maximum correlation value between an individual neuron's GCaMP6 fluorescence signal and the corresponding temperature signal (See Figure 2F).

For TRP mutant CIII (*19-12-Gal4*) and Pkd2 misexpression CIV (*ppk1.9-Gal4*) GCaMP6 imaging, ddaF (CIII) and ddaC (CIV) neurons were recorded at 512 x 512 resolution at 0.31fps on a Zeiss LSM 780. CIII driven GCaMP6 Thermal cycle regiment for GCaMP imaging in TRP mutants: 1. An initial 120 s of 25 ˚C; 2. A ramp down to 6 ˚C at a rate of 20 ˚C/min, holding for 10 s; 3. A ramp up to 25 ˚C at a rate of 20 ˚C/min holding for 60 s. Thermal cycle regiment for GCaMP imaging of Pkd2 misexpression in CIV: 1. An initial 120 s of 25 ˚C; 2. A ramp down to 6 ˚C at a rate of 20 ˚C/min, holding for 10 s; 3. A ramp up to 25 ˚C at a rate of 20 ˚C/min holding for 60 s, followed by a repeat of steps 2 and 3 twice more for a total of three cycles of thermal stimulation/animal. Stats: For TRP mutant GCaMP data, unpaired t-test was used on all genotypic comparisons except for *nompC*^{3}*/Df* mutants where Welch's t-test was performed (See Figure 6B); for Pkd2 misexpression analyses, unpaired t-test was performed (See Figure 6D).

Optogenetics

Third instar larvae expressing *UAS-ChETA-YFP* via class-specific *GAL4* drivers were subjected to optogenetic activation (480 nm) and behavioral responses were recorded on a Nikon D5200 DSLR. For coactivation *19-12-GAL4,UAS-ChETA::YFP* flies were crossed to *GAL4*^{477}*;GAL4*$^{ppk1.9}$ to create progeny bearing ChETA::YFP expression in CIII and CIV neurons. First instar larvae (~24 hours after egg laying) were reared on media with or without 1500 mM of all *trans*-retinal. Optogenetic stimulation consisted of three successive 5 s pulses separated by 10 s periods with no light stimulation. The time (s) that each larva maintained a defined CT response (percent change in body length is above threshold defined above) was measured in 7 s intervals containing the 5 s pulses of blue light stimulation. Reductions in blue light intensities for dose response were achieved by decreasing the aperture on a Zeiss Axio Zoom.V16 stereomicroscope by 10% intervals, while maintaining full larval illumination. Aperture percentage settings were: 100, 90, 80, 70, 60, 50, 40, and 37 corresponding to maximum blue light intensities of 100, 92, 83, 76, 66, 55, 37, and 31 % (Mastech professional luxmeter, range 65 Klx to 20 Klx). The

first behavior observed and maintained in the initial three seconds of blue light stimulation was recorded at each intensity level. Stats: two-tailed Welch's t-test.

CaMPARI

For CaMPARI experiments *19-12-Gal4* was used to drive *UAS-CaMPARI*. Larvae were either subjected to no photoconverting (PC) light or PC light without stimulus, PC light with light touch stimulus, and PC light with cold stimulus. PC light (± stimulus) was briefly delivered to live third instar larvae via a Zeiss AxioZoom.V16 using the same filter set as described in [S15] at 84,000 lux for 20 seconds. Light touch stimulus was delivered using a fine brush bristle mounted on tungsten needle holder, which was found to be sufficient to induce HW behavior. Light touch was first delivered on the head of the larva, followed by a stroke along the anteroposterior axis of the animal under PC light. Cold stimulus (6 ˚C) was delivered as described in the global cold plate assay under PC light. Larvae were imaged as described below. For image analysis, Zeiss Zen Blue Lite was used. Fluorescence change was calculated as previously described [S15] using maximum intensity projections in order to calculate the Fred/Fgreen ratios. Stats: Mann-Whitney U-test.

Cell isolation and qRT-PCR

Neuronal subpopulations were isolated using magnetic-bead-based cell sorting [S7, S8, S21]. Following RNA purification from isolated cells (CIII or CIV md neurons), qRT-PCR and data analyses were performed [S7]. Pre-validated Qiagen QuantiTect Primer Assays (Qiagen, Germantown, MD, USA) were used for: *Pkd2* (QT00935347); *nompC* (QT00930139), and *Trpm* (QT00947261). Expression data were normalized against RpL32 (QT00985677) and are reported as the mean fold change in expression ± s.d comparing CIII to CIV neurons. Stats: Mann-Whitney U-test.

Confocal microscopy and neuromorphometric analyses

For live confocal imaging of neuronal morphology, third instar larvae were immersed in a few drops of 1:5 (v/v) diethyl ether:halocarbon oil and imaged on a Zeiss LSM780 confocal system. Three-dimensional z-stacks were then volume rendered into a two-dimensional maximum projection and resultant images were processed for quantitative neuronal morphological analyses. Quantitative neuromorphometric analyses of dendritic arbors was performed as previously described [S7]. Branch density (number of branches/total length) was compared using a two-tailed Welch's t-test with Bonferonni correction.

Microarray Expression Analyses

Microarray analyses of purified CIII neurons isolated from age-matched third instar larvae were performed [S8]. CIII md neurons (*ppk-Gal4,UAS-mCD8::GFP, ppk-Gal80*) were purified via magnetic bead cell sorting and mRNA was then isolated. mRNA isolation, amplification, labeling, and microarray hybridization were conducted by Miltenyi Biotec. 250 ng of cDNAs were used as a template for Cy3 labeling followed by hybridization to Agilent whole *Drosophila melanogaster* genome oligo microarrays (4x44 K). CIII microarray data, including metadata, raw data, and quantile normalized datasets have been deposited into the Gene Expression Omnibus (GEO) under accession number GSE69353. CIII microarray datasets were compared to our CIV md neuron and whole larval microarray datasets (GSE46154) [S8], which used an identical microarray chip. Statistical analyses of microarray data were performed as previously described [S22].

Raw microarray data files obtained from the Agilent microarrays for class III, class IV, and whole third instar larvae were read into GeneSpring GX software in which the data was quantile normalized and only those gene probes which are flagged positive and significantly expressed above background are selected for further analyses. GeneSpring software was used to calculate mean fold change gene expression where a given gene/isoform was represented by multiple probe IDs on the microarray. Heat maps for the fold change values were constructed using the *gplots* function in *R*. Briefly, fold change values were read into *R* and using the *heatmap.2* function of *gplots* package, which allows for hierarchical clustering of genes based on their relative expression values. Fold-change values were scaled to z-scores (-1 to +1) for data visualization where blue represents down-regulation and yellow represents up-regulation.

Supplemental References

[S1]. Hofmann, T., Chubanov, V., Chen, X., Dietz, A.S., Gudermann, T., and Montell, C. (2010). Drosophila TRPM channel is essential for the control of extracellular magnesium levels. PLoS One *5*, e10519.

[S2]. Walker, R.G., Willingham, A.T., and Zuker, C.S. (2000). A Drosophila mechanosensory transduction channel. Science *287*, 2229-2234.
[S3]. Grueber, W.B., Jan, L.Y., and Jan, Y.N. (2003). Different levels of the homeodomain protein Cut regulate distinct dendrite branching patterns of Drosophila multidendritic neurons. Cell *112*, 805-818.
[S4]. Jenett, A., Rubin, G.M., Ngo, T.T., Shepherd, D., Murphy, C., Dionne, H., Pfeiffer, B.D., Cavallaro, A., Hall, D., Jeter, J., et al. (2012). A GAL4-driver line resource for Drosophila neurobiology. Cell Rep *2*, 991-1001.
[S5]. Xiang, Y., Yuan, Q., Vogt, N., Looger, L.L., Jan, L.Y., and Jan, Y.N. (2010). Light-avoidance-mediating photoreceptors tile the Drosophila larval body wall. Nature *468*, 921-926.
[S6]. Petersen, L.K., and Stowers, R.S. (2011). A Gateway MultiSite recombination cloning toolkit. PLoS One *6*, e24531.
[S7]. Iyer, S.C., Ramachandran Iyer, E.P., Meduri, R., Rubaharan, M., Kuntimaddi, A., Karamsetty, M., and Cox, D.N. (2013). Cut, via CrebA, transcriptionally regulates the COPII secretory pathway to direct dendrite development in Drosophila. J Cell Sci *126*, 4732-4745.
[S8]. Iyer, E.P., Iyer, S.C., Sullivan, L., Wang, D., Meduri, R., Graybeal, L.L., and Cox, D.N. (2013). Functional genomic analyses of two morphologically distinct classes of Drosophila sensory neurons: post-mitotic roles of transcription factors in dendritic patterning. PLoS One *8*, e72434.
[S9]. Ainsley, J.A., Pettus, J.M., Bosenko, D., Gerstein, C.E., Zinkevich, N., Anderson, M.G., Adams, C.M., Welsh, M.J., and Johnson, W.A. (2003). Enhanced locomotion caused by loss of the Drosophila DEG/ENaC protein Pickpocket1. Curr Biol *13*, 1557-1563.
[S10]. Hughes, C.L., and Thomas, J.B. (2007). A sensory feedback circuit coordinates muscle activity in Drosophila. Mol Cell Neurosci *35*, 383-396.
[S11]. Song, W., Onishi, M., Jan, L.Y., and Jan, Y.N. (2007). Peripheral multidendritic sensory neurons are necessary for rhythmic locomotion behavior in Drosophila larvae. Proc Natl Acad Sci U S A *104*, 5199-5204.
[S12]. Sweeney, S.T., Broadie, K., Keane, J., Niemann, H., and O'Kane, C.J. (1995). Targeted expression of tetanus toxin light chain in Drosophila specifically eliminates synaptic transmission and causes behavioral defects. Neuron *14*, 341-351.
[S13]. Chen, T.W., Wardill, T.J., Sun, Y., Pulver, S.R., Renninger, S.L., Baohan, A., Schreiter, E.R., Kerr, R.A., Orger, M.B., Jayaraman, V., et al. (2013). Ultrasensitive fluorescent proteins for imaging neuronal activity. Nature *499*, 295-300.
[S14]. Lee, T., and Luo, L. (1999). Mosaic analysis with a repressible cell marker for studies of gene function in neuronal morphogenesis. Neuron *22*, 451-461.
[S15]. Fosque, B.F., Sun, Y., Dana, H., Yang, C.T., Ohyama, T., Tadross, M.R., Patel, R., Zlatic, M., Kim, D.S., Ahrens, M.B., et al. (2015). Neural circuits. Labeling of active neural circuits in vivo with designed calcium integrators. Science *347*, 755-760.
[S16]. Cheng, L.E., Song, W., Looger, L.L., Jan, L.Y., and Jan, Y.N. (2010). The role of the TRP channel NompC in Drosophila larval and adult locomotion. Neuron *67*, 373-380.
[S17]. Hamada, F.N., Rosenzweig, M., Kang, K., Pulver, S.R., Ghezzi, A., Jegla, T.J., and Garrity, P.A. (2008). An internal thermal sensor controlling temperature preference in Drosophila. Nature *454*, 217-220.
[S18]. Dietzl, G., Chen, D., Schnorrer, F., Su, K.C., Barinova, Y., Fellner, M., Gasser, B., Kinsey, K., Oppel, S., Scheiblauer, S., et al. (2007). A genome-wide transgenic RNAi library for conditional gene inactivation in Drosophila. Nature *448*, 151-156.
[S19]. Ni, J.Q., Markstein, M., Binari, R., Pfeiffer, B., Liu, L.P., Villalta, C., Booker, M., Perkins, L., and Perrimon, N. (2008). Vector and parameters for targeted transgenic RNA interference in Drosophila melanogaster. Nat Methods *5*, 49-51.
[S20]. Babcock, D.T., Landry, C., and Galko, M.J. (2009). Cytokine signaling mediates UV-induced nociceptive sensitization in Drosophila larvae. Curr Biol *19*, 799-806.
[S21]. Iyer, E.P., Iyer, S.C., Sulkowski, M.J., and Cox, D.N. (2009). Isolation and purification of Drosophila peripheral neurons by magnetic bead sorting. J Vis Exp.
[S22]. Bhattacharya, S., Iyer, E.P., Iyer, S.C., and Cox, D.N. (2014). Cell-type specific transcriptomic profiling to dissect mechanisms of differential dendritogenesis. Genom Data *2*, 378-381.